Delayed paced ventricular activation in the long QT syndrome is associated with ventricular fibrillation

Richard C. Saumarez, PhD, FRCP[*,†,‡] Mariusz Pytkowski, MD,[§] Maciej Sterlinski, MD,[§] Richard N. W. Hauer, MD,[¶] Richard Derksen, MD,[¶] Martin D. Lowe, MB, PhD,[*†] Hannah Szwed, MD,[§] Christopher L.-H. Huang, MD, ScD,[‖] David E. Ward, MD, FRCP,[**] A. John Camm, MD, FRCP,[**] Andrew A. Grace, PhD, FRCP[*,†]

*From the Department of Cardiology, Papworth Hospital, †Department of Biochemistry, University of Cambridge, ‡Department of Engineering, University of Cambridge, Cambridge, United Kingdom, §Institute of Cardiology, Warsaw, Poland, ¶Heart Lung Center Utrecht, University Medical Center, Utrecht, The Netherlands, ‖Physiological Laboratory, University of Cambridge, Cambridge, United Kingdom, and **Department of Cardiological Sciences, St. George's Hospital Medical School, London, United Kingdom.*

BACKGROUND LQTS may cause sudden cardiac death (SCD), but the mechanisms linking gene mutations to ventricular fibrillation (VF) are unclear.

OBJECTIVE To determine whether ventricular activation delays in congenital long QT syndrome (LQTS) are associated with VF and to describe these delays clinically by measuring activation through ventricular myocardium after a premature extrastimulus.

METHODS Forty-six patients with LQTS, including 16 with VF (LQTS VF) were investigated, and the results were compared with those from 24 patients with hypertrophic cardiomyopathy and VF (HCM VF). Electrograms in response to premature stimuli were analyzed for increases in electrogram duration (ΔED) and the S1S2 coupling intervals at which electrogram latency starts to increase ($S1S2_{delay}$). Two piecewise continuous straight line segments were fitted to the last electrogram deflection as a function of S1S2 interval in the LQTS and HCM VF populations, and the difference in their gradient (α) was taken as an index of the abruptness of the onset of this delay.

RESULTS Thirteen LQTS VF and six LQTS non-VF patients had values of ΔED and $S1S2_{delay}$ comparable to those in HCM VF patients, while the remainder (three LQTS VF and 24 LQTS non-VF) had lower values ($P<.001$). There was only a weak correlation between delay and the corrected QT interval. The HCM and LQTS VF patients could be separated by the value of α ($P<.01$), with the LQTS patients having a more abrupt onset of delay.

CONCLUSIONS Large delays in ventricular activation after an extrastimulus occur in patients with the LQTS, especially those with VF. The change in delay is abrupt in the LQTS, indicating sudden block to activation creating a dynamic substrate for arrhythmogenesis.

KEYWORDS Cardiac arrest; Long QT syndrome; Electrophysiology; Arrhythmia; Torsade de pointes

(Heart Rhythm 2006;3:771–778)

Noncoronary heart disease that alters myocardial structure or function predisposes to ventricular fibrillation (VF) and sudden cardiac death (SCD).[1] Although arrhythmias in congenital long QT syndrome (LQTS) are linked to mutations in genes encoding ion channel subunits[2,3] or supporting structural proteins,[4] the exact mechanisms of SCD in this disease remain unclear.[3]

The initiation of reentrant tachycardias requires a substrate of one or more areas of slowed conduction and activation block.[5] In classical, well-characterized reentrant arrhythmias, slowed conduction and activation block can be inferred from the activation sequence of induction, reset, or termination of the arrhythmia by precisely timed extrastimuli.[5–7] In contrast to these arrhythmias with a specific anatomical substrate, reentrant VF arising from a functional substrate created by a dynamically changing pattern of refractoriness and activation[8] has proven difficult to study clinically. Against this background, paced electrogram fractionation analysis (PEFA) was developed[9] to identify a substrate for VF by timing the activation of ventricular sites in response to increasingly premature extrastimuli. This technique is based on the hypothesis that diseased tissue, which might contain a substrate for VF, would show fractionated potentials with increasing delay within recorded electrograms ("fractionation") created by tortuous activation paths around fibrous or functionally altered tissue and that these effects could be accentuated by local conduction block as the extrastimulus coupling interval was reduced.[7]

This work was supported by the British Heart Foundation and EC Biomed contract no. BMH4 96 1088. **Address reprint requests and correspondence:** Dr. R.C. Saumarez or Dr. A.A. Grace, Department of Cardiology, Papworth Hospital/University of Cambridge, Cambridge CB3 8RE, United Kingdom. E-mail address: ag@mole.bio.cam.ac.uk (Received August 29, 2005; accepted March 10, 2006.)

1547-5271/$ -see front matter doi:10.1016/j.hrthm.2006.03.013

Table 1 Details of patients in the study

Feature	LQTS	LQTS VF	Controls
Gender F/M	23F/7M	14F/2M	5F/7M
Age (years)			
20<	8	6	2
20-40	14	7	7
40-60	8	3	3
PEFA:			
Negative/positive	24/6	3/13	
QTc			
<0.44			12
0.46	3	1	
0.46-0.5	8	0	
0.5-0.55	15	5	
>0.55	4	10	
Syncope	2	0	
Torsades des Pointes	4	0	
Number with ICDs	8	2 prior to VF 13 post VF	

This hypothesis has been tested in more than 500 patients with a variety of noncoronary diseases, and an association between the risk of VF and electrogram fractionation has been found in hypertrophic cardiomyopathy (HCM), dilated cardiomyopathy (DCM), LQTS, and idiopathic VF.[1,10,11] While these studies have shown that there is a physiological effect that is compatible with the presence of a substrate for VF, it may have a number of disease-specific mechanisms. The structural changes described in HCM such as fibrosis and disarray[12] are likely to create delays due to tortuous conduction and local block effects exacerbated by dispersion of the action potential duration.[13] In contrast to such structural heart disease, LQTSs have normal myocardial architecture, and it is surprising, at first sight, that there should be activation delays at all. These delays are presumably the result of functional electrophysiological changes,[14,15] and in this paper we show that there is markedly delayed ventricular activation in the LQTS associated with SCD. Also, the nature of the delays is different from that seen in HCM VF and suggests that activation block is occurring in refractory tissue, leading to tortuous and delayed activation.

Methods

Patients

All Local Research Ethics Committees approved the study protocol, and patients gave informed written consent for this investigational study. The details of the patients are shown in Table 1: (1) 46 consecutive patients (eight males) aged 11–56 years with congenital LQTS diagnosed based on standard criteria[16] were studied (Table 1). Of these, (a) 14 patients were studied at some point after resuscitation from VF and (b) a further two patients received an appropriate ICD discharge some months after their electrophysiological studies. All but one patient was implanted with an ICD after resuscitation from VF. (c) Of the 30 non-VF patients, four had documented torsades de pointes (TdP) and two had syncope. All patients have been treated with beta blockade and eight patients, including those with TdP and syncope, have had implantable cardioverter-defibrillators (ICDs) implanted. While these patients continue to be followed up, no ICD has discharged to date. (2) The 12 controls have been previously described as have (3) the 24 patients with HCM and VF that were obtained contemporaneously and were used as a comparison group with the LQTS VF patients.[1]

Electrophysiological methods

The technique has been described in earlier publications.[9,10,11,17] In drug-free patients, four, 1 cm spaced, electrode catheters were positioned at different sites in the right ventricle and a pacing sequence delivered from one catheter with electrograms recorded at the remaining sites (Figure 1). The sequence is a two-stimulus drive train with an interstimulus interval of 490 ms and an extrastimulus delivered every third beat, and the extrastimulus-coupling interval (S1S2 interval) is reduced in 1 ms steps from 450 to 220 ms or the refractory period. The electrogram signals were digitized from each catheter during this process with 16-bit precision at a sampling rate of 1 kHz.

After the study, the data were analyzed in a number of steps as detailed in the lettering in Figure 1. The first step is to identify each discrete potential within an electrogram in response to an extrastimulus and to achieve a robust separation between the signal and the noise (Figure 1, step A). The method used is an established technique for identifying a signal in the presence of noise known as a matched, or noise-reduction, filter.[18,19] A template that resembles a feature in the signal that is to be identified is correlated with the signal in question. Where there is a component in the signal that matches the template, there will be a high correlation output from the filter at an identical time to the time of the feature in the signal. Conversely, if the signal is entirely noise, there will be no correlation between the template and signal. Peaks in the electrogram, between 10 and 190 ms after the stimulus, are detected by using a matched filter with templates that resemble deflections within an electrogram. These identify the positions of peaks in the electrogram and fail to do so in regions that are noise. This is shown in Figure 1, step B, where a noisy signal with two deflections in it is correlated with the template that resembles an electrogram potential. The matched filter output shows distinct peaks at the positions of the potentials and a low output in regions that are simply noise. The matched filter outputs in the region 200–450 ms after stimulus are assumed to be entirely due to noise and are taken as a threshold for peak detection in the earlier portion of the signal. In practice, several electrogram templates of different widths are used and are correlated with the signal to be certain of identifying peaks of different widths. This technique identifies, in particular, the first and last potential in the electrogram, so yielding the electrogram duration. However, intermediate points between the first and last are not included in this analysis.

The second step in the processing is generation of conduction curves that describe how activation changes, as the

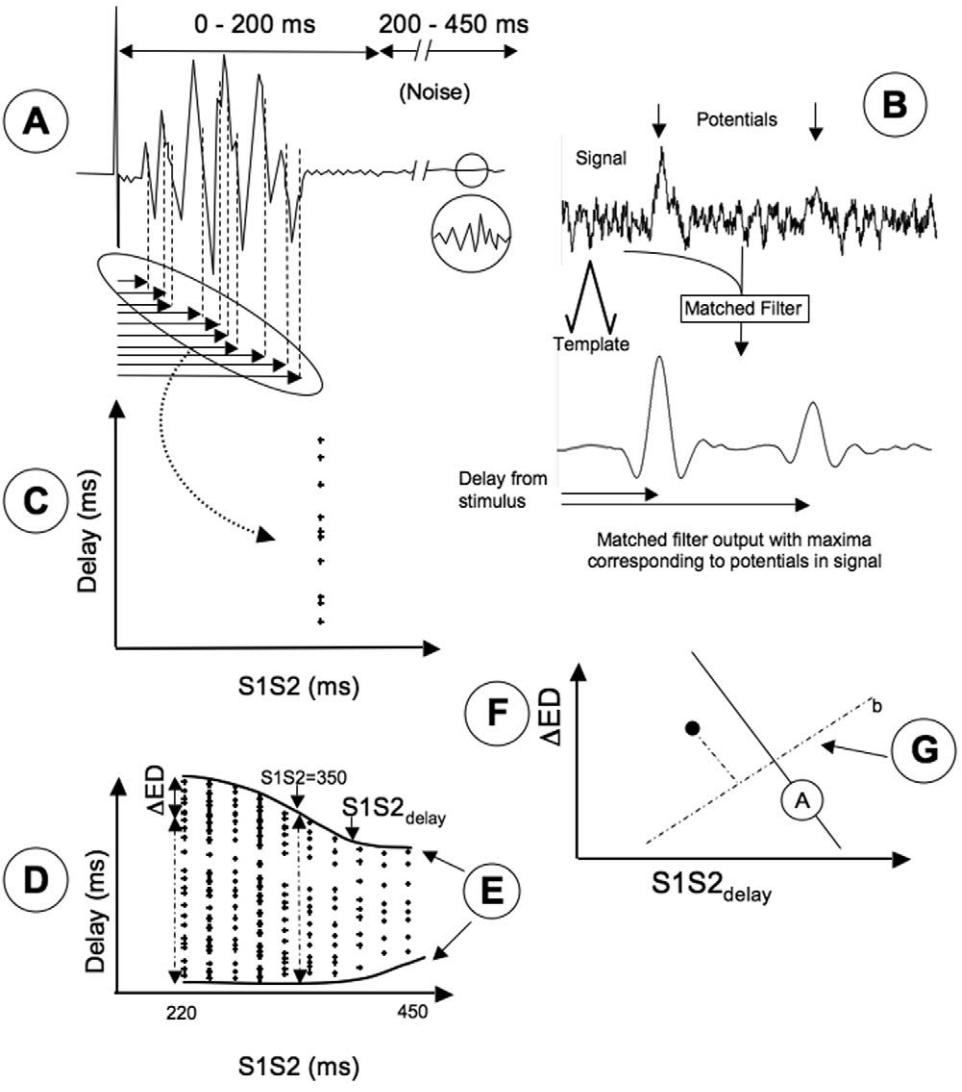

Figure 1 A diagram showing how the raw electrograms obtained during a study are analyzed to yield a measure of risk of SCD. **A**: An electrogram after an extrastimulus is processed by identifying maximum negative derivatives and their delay after the stimulus. The terminal portion of the trace (200–450 ms) is used to determine the noise. **B**: Simplified description of identification of electrogram potentials from noise. The simulated signal contains two potentials (*arrowed*), and noise is added to the signal. The signal and the template of an electrogram potential are correlated in the matched filter to give an output. The maxima correspond to the potentials embedded in the noisy signal. Note that the second, low-amplitude, potential is practically indiscernible in the signal but is identified by the matched filter output. In practice, a number of templates of different widths are used to distinguish potentials of different lengths. The threshold of accepting a peak in the matched filter output is determined by calculating the peak value of the output in the region of 200–450 ms poststimulus, which is assumed to be solely noise. **C**: The delays after the extrastimulus are plotted against the S1S2 interval at which the electrogram was recorded. **D**: This is repeated for all the electrograms recorded between S1S2s of 450 and 220 ms creating the "conduction curve" of the kind illustrated in Figure 3. **E**: The curves are characterized by fitting splines to their upper and lower boundaries. This allows measurement of the change in electrogram duration (ΔED) and the critical point at which delay starts to increase ($S1S2_{delay}$). **F**: The values of $S1S2_{delay}$ and ΔED for all the pacing runs are averaged and plotted as a single observation (Figures 4 and 5). The high-risk region is in the top right corner, and the low-risk region (i.e., controls) is in the bottom left (Figure 4). Line A in the diagram is the line determined retrospectively to separate high-risk and low-risk patients. **G**: The positions of all patients are projected onto line b (at 90° to line A). These are rotated so that line b forms the x-axis of Figure 6. Details of data acquisition are described in the Methods section.

S1S2 interval is decreased and forms a visual interpretation of activation and risk. These are formed by plotting the delays of detected potentials in an electrogram against the S1S2 interval at which the electrogram was obtained (Figure 1, step C), and this is repeated for all the electrograms in the pacing run (Figure 1, step D). These are shown in Figure 3, and each cross in a plot represents the delay of a detected potential at a particular S1S2.

These conduction curves are reduced to two parameters for further analysis. One is thought to represent the capacity of the tissue to generate delayed conduction, that is, a substrate and is the increase in electrogram duration between an S1S2 of 350 ms and 5 ms above VERP (ΔED). The second is the S1S2 at which the electrogram duration starts to increase ($S1S2_{delay}$). This is thought to be a measure of vulnerability since electrogram prolongation at a long S1S2 might represent exposure of a substrate, that is, delay, by a relatively minor stimulus and so present a risk of VF. Electrogram prolongation that occurs at short S1S2 intervals may be difficult to provoke and occur rarely, thus making the patient at low risk of SCD. In practice, these variables are difficult to measure directly off many curves,

which do not have absolutely smooth boundaries. To get a stable estimate of ΔED and $S1S2_{delay}$, cubic splines are fitted by an automated method to the upper and lower boundaries of the curve and the electrogram duration is calculated at any S1S2 from the splines (Figure 1, step E). The $S1S2_{delay}$ is obtained by differentiating the spline fitted to the upper boundary of the curve and its value is taken as the S1S2 interval at which its derivative decreases below a threshold gradient (−0.05 ms/1 ms increase in S1S2 interval) that was determined in earlier studies.[9] The mean of these values for all the runs for a patient is then plotted as a single observation on a scattergram of ΔED versus $S1S2_{delay}$ (Figure 1, step F) as shown in Figure 4. The hypothetically highest-risk category, with maximum fractionation, is in the top right-hand corner and the lowest-risk category is in the bottom left-hand corner. The discriminant line A is the line constructed from the initial series of 101 patients that distinguishes VF and non-VF HCM patients[10] and has been slightly modified in the light of improved signal processing methods,[17] which have been applied retrospectively to all the data presented in this paper.

Statistical analysis

The probability of the LQTS VF patients conforming to the HCM VF group and LQTS non-VF patients segregating with the low-risk HCM group[10] was calculated using the discriminant line A in Figure 4 with Fisher's exact test. To test the hypothesis that conduction in the LQTS is normal above a particular S1S2 after which there is a sudden onset of long activation delays, two piecewise continuous straight-line segments were fitted, by minimum sum of squared error, to the upper boundary of the conduction curve (Figure 3). This conforms to the feature of the LQTS curves in that they are flat until a threshold S1S2 is reached and they then show a sharp increase in delay as the S1S2 interval is further reduced. In HCM, the curves generally show a gradual increase in delay without sharp inflections. This is quantified by the angle between the fitted straight-line segments, α (which is smaller and more acute for the LQTS) and the mean value for each patient was obtained. The subsequent description of the patient in terms of $S1S2_{delay}$, ΔED, and α was used to find the discriminant plane, which maximally separated the LQTS VF and HCM VF patients into distinct groups. This was almost entirely due to α, and these are plotted for the HCM and LQTS VF patients and are shown in Figure 6. The probability of this separation was computed by the rank-sign test as $<.005$.

To examine the relationship between the corrected QT (QTc) and fractionation, the results in Figure 4 are further manipulated to form a single index of risk. They are reduced to the projection of the point along a line that is normal to the discriminant line A shown in Figures 1G (line b), 4, and 5. This line then becomes the abscissa of Figure 5 with the QTc as the ordinate. The units are in milliseconds, and controls (not shown) range from 0 to 6; 100 is very intense fractionation, and line A, defined in Figure 4, is at 60.

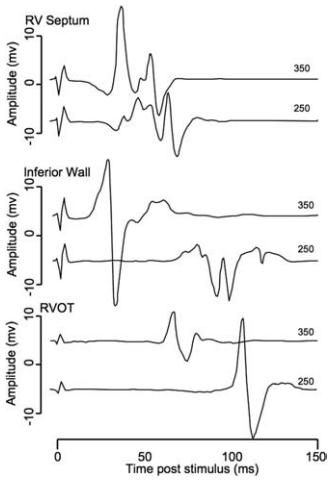

Figure 2 Bipolar electrograms recorded from an LQTS VF survivor at S1S2 intervals of 350 and 250 ms. The electrograms show large delays and also the delays in each channel change relative to each other at a shorter S1S2 interval. This demonstrates that the delays are not due to a delay at the stimulating electrode or stimulus-to-tissue latency.

Results

This section describes in sequence, beginning from the electrogram traces that form their basis, results from the sequence of electrophysiological analysis or statistical procedures described in the Methods section above. Thus, Figure 2 shows a set of electrograms obtained at S1S2 coupling intervals of 350 and 250 ms from a patient with LQTS who had survived VF. The right ventricular (RV) apex was paced with electrograms recorded from the RV septum, RV inferior wall, and RV outflow tract. Electrograms obtained from the septum and inferior wall at an S1S2 coupling interval of 250 ms are fractionated as they are delayed, are longer, and have an increased number of potentials compared with those obtained with an S1S2 of 350 ms. The interval between electrograms recorded at 350 and 250 ms differs in this patient at each site, showing that the imposed delays are due to activation through myocardium rather than to increased stimulus-to-tissue latency and that the activation sequence has changed.

Traces of the kind described above formed the basis of the conduction curves that described changes in delays of detected electrogram potentials with decreasing S1S2 interval, thereby providing a visual representation of interpretation of activation and risk from any given patient. Such an analysis is effectively confined to the envelope defined by the first and last electrograms; in its present form, it does not quantitatively represent the remaining deflections. Nevertheless, these plots of the increase in electrogram duration between an S1S2 of 350 and 5 ms above VERP (ΔED) have been previously suggested to represent the capacity of the tissue to generate delayed conduction against the S1S2 at which the electrogram duration starts to increase ($S1S2_{delay}$), which is thought to be a measure of vulnerability. Figure 3 shows representative curves taken from three LQTS and three HCM VF patients. All the curves from the LQTS and HCM show a pattern associated with

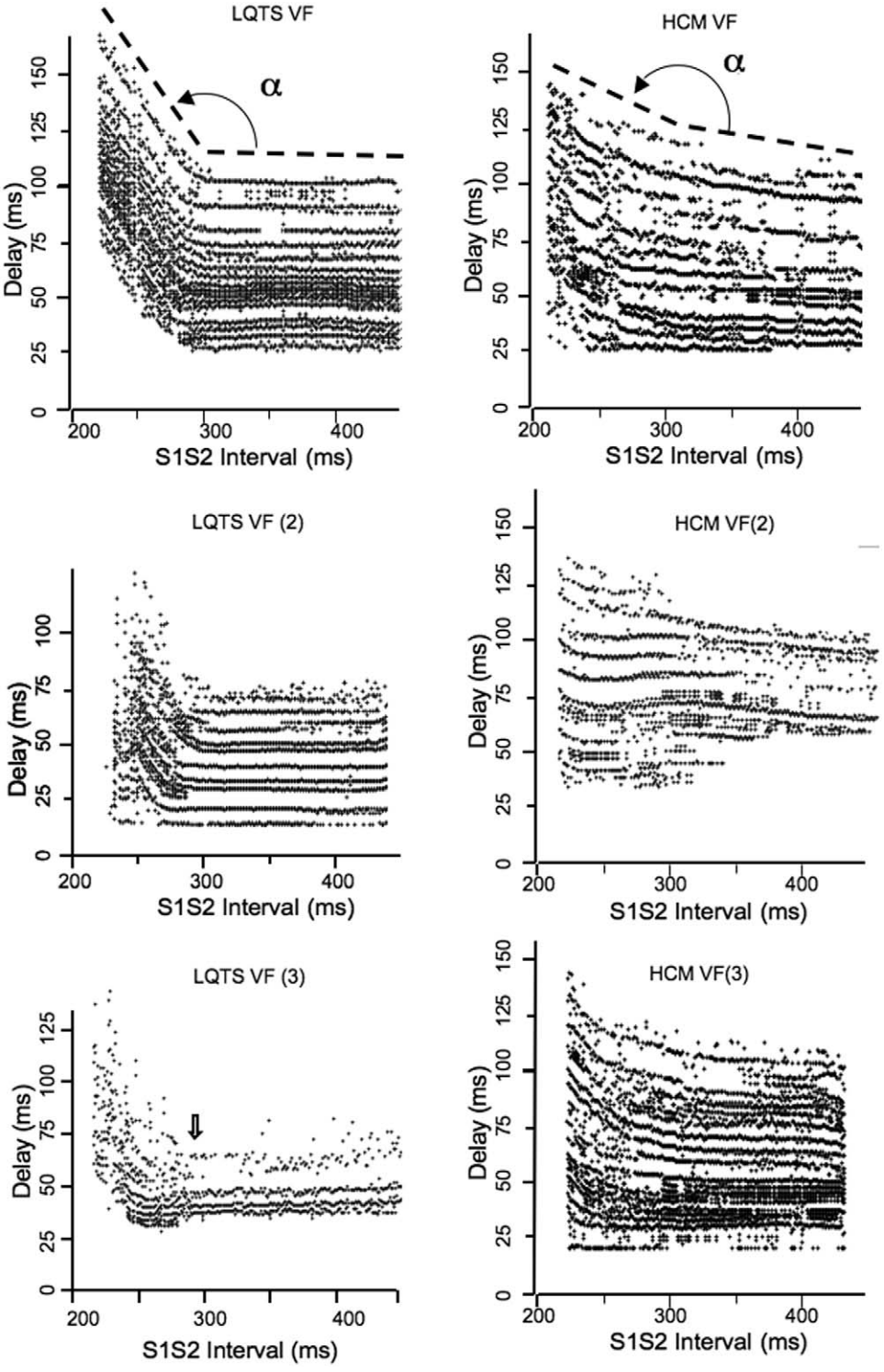

Figure 3 Conduction curves obtained from typical examples of three LQTS VF survivors and three HCM VF survivors. The abrupt change in delay in the LQTS is illustrated, while the delay increases gradually in the HCM patient. The piecewise continuous set of two lines fitted the upper boundary of the curves are shown (elevated for clarity) as is the angle α between the two segments.

VF: the electrogram duration, as shown by the upper and lower limits in delay at a particular S1S2 interval, is markedly increased close to VERP, and this increase started to occur at S1S2 intervals of 280–300 ms in the LQTS and above 400 ms for HCM. These values are higher than controls where the S1S2 interval at which electrograms start to prolong is typically 240–260 ms. However, the LQTS VF patients have a different form from that in HCM with curves that do not change until a threshold S1S2, below which there is an abrupt increase in electrogram delay. In HCM, there is a gradual increase in electrogram delay with a changing pattern of activation and this starts at longer S1S2 intervals. The pairs of straight lines fitted to the upper boundary of the curve are shown, elevated above the curves for clarity, and the angles α between them, used to quantify the change in the shape of the curve, are also shown. In

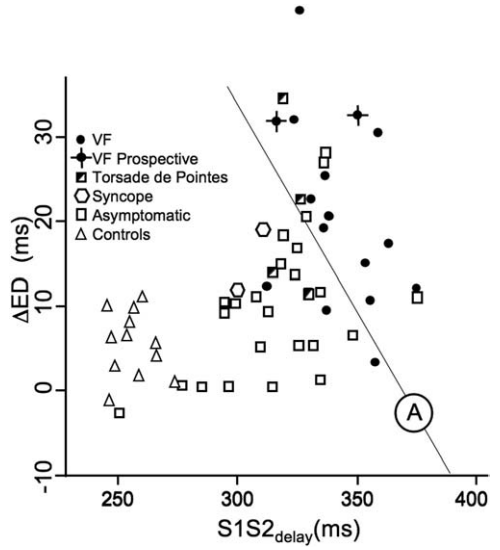

Figure 4 Scattergram of mean ΔED against mean $S1S2_{delay}$ for LQTS VF, non-VF, and control patients. The symbol for each category of patient is shown on the graph. The discriminant line A is that which was constructed to distinguish between HCM VF and non-VF patients and shows that the delays seen in the LQTS are comparable to those in HCM. The majority of VF patients (13/16) lie in the high-risk region as opposed to 6/30 non-VF patients. The 12 controls cluster in the lower left corner of the plot, indicating minimum disturbance.

these examples it is clear that the value of α is smaller in the case of the LQTS when compared with that of the HCM curve.

The discriminant line separating HCM VF and HCM non-VF patients, which was obtained from earlier studies, is used to distinguish LQTS VF and non-VF patients (Figure 4). Thirteen of 16 LQTS VF and six of the 30 LQTS non-VF patients lie to the right of this line, while only thee LQTS VF and 24 LQTS non-VF patients lie to the left of line A ($P<.001$, Fisher's exact test). By contrast, controls show very little change in electrogram duration and this occurs at a shorter S1S2 interval than all but one of the LQTS patients. The positions of the LQTS patients and controls plotted on a scattergram of ΔED against $S1S2_{delay}$ and the discriminant line separating VF and non-VF HCM patients is shown as line A.

In contrast, there is only a weak correlation between the degree of fractionation and the QTc. This is illustrated in the scattergram in Figure 5. The correlation coefficient between QTc and fractionation is 0.28, corresponding to a $P>.05$, which is borne out by the wide spread of QTc values for a given fractionation value. By the same token, fractionation identifies 13/16 VF patients with six non-VF patients, while a cutoff in QTc that identifies 12/16 patients (QTc = 510 ms) also identifies 17 non-VF patients. Thus the association between fractionation and QTc is weak.

These findings contrast with the results in Figure 6, which shows the mean values of α, which is the angle between the two piecewise continuous lines fitted to the upper border of the curve for each HCM and LQTS VF patient. It is clear that the LQTS patients have a more abrupt onset of delay than the HCM patients and that there is a significant discrimination between the two groups ($P<.005$).

Discussion

This study demonstrates delays in paced myocardial activation in LQTS and then goes on to associate the magnitude of such delays with the clinical risk of VF. It thereby complements findings in VF patients with HCM and DCM and also suggests that activation delay after a premature stimulus reveals the arrhythmogenic substrate for VF, regardless of the disease,[1] and that intense electrogram fractionation can occur even in structurally normal hearts. Such observations suggest that fractionation and induction of VF is produced by functional block of activation, or by contrasting mechanisms for arrhythmogenesis suggested specifically for LQTS, rather than anatomical obstruction.

Nevertheless, some of the differences between conduction curves obtained from LQTS and HCM patients might reflect some of the differences in the mechanisms of the conduction delay. Those in the LQTS VF patients were normal at the longer S1S2 intervals but below a threshold S1S2 interval showed an abrupt and large increase in delay with a variable number of potentials in each delayed electrogram. These data thus approximated two piecewise continuous straight line segments separated by an angle, α, between the segments that was considerably more abrupt in the LQTS compared with the HCM patients. These findings are compatible with a scheme in which ventricular conduction after an extrastimulus is normal in LQTS until the S1S2 interval is reduced to a point where some areas of the myocardium are still refractory after the last drive train stimulus. There is then a dynamic block to activation re-

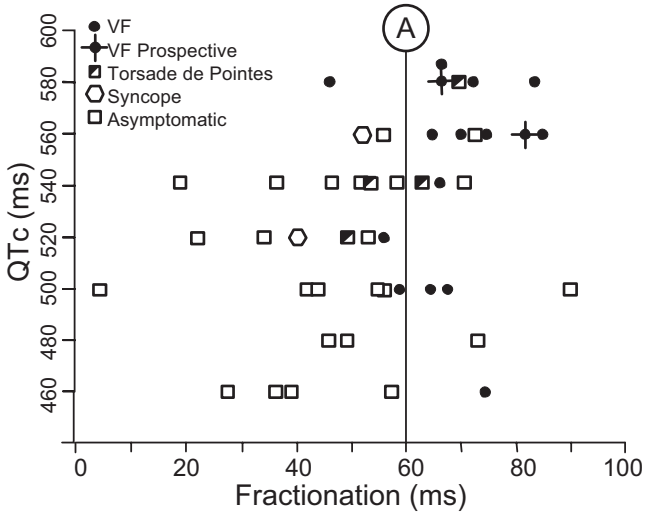

Figure 5 A scattergram of fractionation (as defined in statistics section of the main text) against QTc. This is created by a projection of each mean observation onto a line that is at 90° to line A in Figures 4 and 5 (see Figure 1G). This transforms each two-dimensional observation into a single value indicator of fractionation. The value of the resting QTc (rounded to the nearest 20 ms) is then plotted against this. Line A is the transformed line A shown in Figure 4.

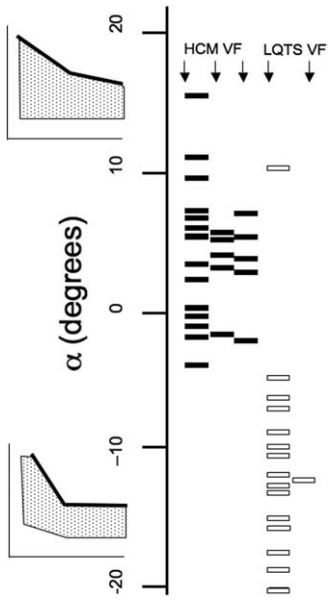

Figure 6 Scatter of α for HCM and LQTS VF patients showing maximum separation between the 2 groups. The axis is change in electrogram delay (α) from the population mean, illustrating the fact that the LQTS (negative) has a more abrupt onset of delay than does HCM (positive).

sulting in delayed and fractionated potentials as wave fronts find paths in the repolarized and relatively refractory tissue that surrounds the refractory area.

Similar effects have been reproduced in mathematical models of myocardial excitation. These had demonstrated that a reduction in I_{Kr} and 5% dispersion of its activity produce conduction curves similar to those obtained in man.[20] Similar findings are also shown in activation maps obtained from anthopleurin A–treated canine hearts[14,21] and hypertrophied hearts after complete heart block and perfusion with dofetilide.[22] In both these experimental LQTS models, paced stimuli led to normal rapid activation but premature ventricular stimuli, equivalent to an extrastimulus in our study, that subsequently led to TdP and resulted in markedly delayed activation down abnormal routes determined by the functional block. Optical mapping in the Kv1.1 genetically modified mouse similarly shows functional block and delayed, circuitous conduction after an S2 stimulus.[23] Further evidence supporting the direct connection between ion channel function and delayed myocardial activation has been obtained in both the Langendorff-perfused, isolated mammalian heart perfused with dofetilide,[17] and in genetically modified mouse. hearts[15,24] These studies used pacing and analysis protocols that were similar to those adopted in the present clinical studies and yielded conduction curves strikingly similar to the human LQTS curves. The genetically modified mouse models additionally develop arrhythmias,[15,24] suggesting, particularly in the case of homozygous disruption of KCNE1, a direct relationship between fractionated potentials and arrhythmias.[15] While arrhythmias in such models may not fully reflect human disease, these models are consistent with the hypothesis that we have advanced to explain data obtained from man, and they support the concept that delayed fractionated potentials reveal some components of the arrhythmic substrate created by prolonged repolarization.

The results from patients with HCM suggest other mechanisms that delay activation apart from repolarization abnormalities. First, "zig-zag conduction" within disarrayed, fibrotic tissue will cause delays and fractionated electrograms as activation waves traverse a number of potential paths. Depending on their refractory periods, some of these may be blocked after an extrastimulus and so will, again, create fractionated electrograms.[25] Second, the inability to support rapid expansion of a wave front when escaping from an aperture in fibrous tissue[26] has been shown to cause delayed conduction in highly fibrotic hearts and this may also happen in HCM.[7,27] These effects have been shown in mathematical models[20] to cause delays at a range of S1S2 intervals and may account for the gradual increase in delay with decreasing S1S2 intervals seen in HCM. Irrespective of the mechanism, the effects of fibrosis and altered repolarization in HCM on ventricular activation are distinguishable in man from those seen in LQTS, suggesting the existence of two different types of arrhythmogenic substrate.

Tridimensional mapping[14,22] shows that TdP may have an intramural initiation and activation sequence and so its critical substrate may be in the M cell layer or its junction with epicardial cells.[21] Since our measurements are endocardial, it is not possible to distinguish how much of an intramural substrate would be within the receptive fields of the electrodes. However, some of the measured delayed potentials are small, in the order of 15 μV, and it is possible that these arise from the intramural components of the substrate that are on the edge of the receptive field of the electrode. In view of the clear separation between VF and non-VF patients, it would appear that the endocardium contains a component of a VF substrate, even if some of the arrhythmic substrate may reside deeper within the ventricular wall.

The relationship between PEFA and the QTc is not as direct as might be thought, and they do not appear to measure identical effects. The data in Figure 5 show clearly that there is only a weak relationship between the magnitude of fractionation and QTc with a correlation coefficient of 0.28. As PEFA identified 13/16 VF patients with six non-VF patients, while a cutoff in QTc that identifies 12/16 patients (QTc = 510 ms) also identifies 17 non-VF patients, it may have a higher predictive accuracy than QTc. The discrepancy between PEFA and QTc is probably because the QTc measures repolarization over a large area of the heart in sinus rhythm in which there is generally recovery from the preceding beat while PEFA measures how conduction, as influenced by repolarization, varies as a small region of tissue becomes increasingly refractory after increasingly premature extrastimuli. This difference illustrates the underlying idea of the relationship between PEFA and risk of SCD: VF rarely arises spontaneously during resting sinus rhythm but arises when the heart is stressed in

some way by, for example, a premature beat or associated with exercise. PEFA is designed to stress the heart with extrastimuli in a way that will bring out slowed and dispersed conduction and, for this reason, it reveals different information to the QTc.

The long delays after an extrastimulus help to understand the development of VF in the LQTS. It is known from ambulatory ECG recordings and data from implantable defibrillators that many cases of TdP organize into a more ordered arrhythmia and terminate. A number of cases will degenerate into VF and cause SCD,[3] and the results of this study suggest a cause. During TdP, the myocardium is activated with rapid, repetitive wave fronts, which would, on the basis of PEFA and animal mapping data, be likely to cause intermittent block and lacunae of repolarizing tissue that would be susceptible to invasion and potentially reentry. This process is more likely to occur when there is a wide and delayed distribution in activation times in the tissue which increases the "window" in which delayed activation fronts may meet repolarized tissue, and this is borne out by the strong association between the duration (ΔED) of electrograms and the occurrence of VF in our patient population.

Our results strongly suggest that PEFA, unlike programmed electrical stimulation,[29] may have a role in the management of the LQTS and could be used for risk stratification, especially in relatives of patients with SCD who have a marked ECG phenotype.[30] The use of such testing in risk stratification is logical as it exposes some components of the mechanisms for lethal arrhythmias and is therefore likely to enhance other methods based on, for example, ECGs, mutational analysis, and gender.[16] While our data show that there is an effect, which is associated with SCD comparable to that seen in HCM and DCM, this is a descriptive study, and the analysis has been performed using criteria that were developed for HCM, which may not be ideal for the LQTS. Nevertheless, this preliminary study now justifies a prospective trial of the PEFA technique in the LQTS, which would give a clearer idea of the clinical significance of the observations presented here.[28]

References

1. Saumarez RC, Chojnowska L, Derksen R, Pytkowski M, Sterlinski M, Huang CL, Sadoul N, Hauer RN, Ruzyllo W, Grace AA. Sudden death in noncoronary heart disease is associated with delayed paced ventricular activation. Circulation 2003;107:2595–2600.
2. Keating MT, Sanguinetti MC. Molecular and cellular mechanisms of cardiac arrhythmias. Cell 2001;104:569–580.
3. Vincent GM. Risk assessment in long QT syndrome: the Achilles heel of appropriate treatment. Heart Rhythm 2005;2:505–506.
4. Mohler PJ, Schott JJ, Gramolini AO, Dilly KW, Guatimosim S, duBell WH, Song LS, Haurogne K, Kyndt F, Ali ME, Rogers TB, Lederer WJ, Escande D, Le Marec H, Bennett V. Ankyrin-B mutation causes type 4 long-QT cardiac arrhythmia and sudden cardiac death. Nature 2003;421:634–639.
5. Janse MJ, Downar E. Reentry. In: Rosen MR, ed. Foundations of cardiac arrhythmias. Basic and clinical approaches. New York: Marcel Dekker, 2001: 449–477.
6. Josephson ME. Electrophysiology of ventricular tachycardia: an historical perspective. J Cardiovasc Electrophysiol 2003;14:1134–1148.
7. Derksen R, van Rijen HV, Wilders R, Tasseron S, Hauer RN, Rutten WL, de Bakker JM. Tissue discontinuities affect conduction velocity restitution: a mechanism by which structural barriers may promote wave break. Circulation 2003;108:882–888.
8. Jalife J. Ventricular fibrillation: mechanisms of initiation and maintenance. Ann Rev Physiol 2000;62:25–50.
9. Saumarez RC, Camm AJ, Panagos A, Gill JS, Stewart JT, de Belder MA, Simpson IA, McKenna WJ. Ventricular fibrillation in hypertrophic cardiomyopathy is associated with increased fractionation of paced right ventricular electrograms. Circulation 1992;86:467–474.
10. Saumarez RC, Slade AK, Grace AA, Sadoul N, Camm AJ, McKenna WJ. The significance of paced electrogram fractionation in hypertrophic cardiomyopathy. A prospective study. Circulation 1995;91:2762–2768.
11. Saumarez RC, Heald S, Gill J, Slade AK, de Belder M, Walczak F, Rowland E, Ward DE, Camm AJ. Primary ventricular fibrillation is associated with increased paced right ventricular electrogram fractionation. Circulation 1995;92:2565–2571.
12. Varnava AM, Elliott PM, Baboonian C, Davison F, Davies MJ, McKenna WJ. Hypertrophic cardiomyopathy: histopathological features of sudden death in cardiac troponin T disease. Circulation 2001;104:1380–1384.
13. Tomaselli GF, Marban E. Electrophysiological remodeling in hypertrophy and heart failure. Cardiovasc Res 1999;42:270–283.
14. El-Sherif N, Chinushi M, Caref EB, Restivo M. Electrophysiological mechanism of the characteristic electrocardiographic morphology of torsade de pointes tachyarrhythmias in the long-QT syndrome: detailed analysis of ventricular tridimensional activation patterns. Circulation 1997;96:4392–4399.
15. Balasubramaniam R, Grace AA, Saumarez RC, Vandenberg JI, Huang CL. Electrogram prolongation and nifedipine-suppressible ventricular arrhythmias in mice following targeted disruption of KCNE1. J Physiol 2003;552:535–546.
16. Priori SG, Schwartz PJ, Napolitano C, Bloise R, Ronchetti E, Grillo M, Vicentini A, Spazzolini C, Nastoli J, Bottelli G, Folli R, Cappelletti D. Risk stratification in the long-QT syndrome. N Engl J Med 2003;348:1866–1874.
17. Saumarez RC, Grace AA. Paced ventricular electrogram fractionation and sudden death in hypertrophic cardiomyopathy and other non-coronary heart diseases. Cardiovasc Res 2000;47:11–22.
18. Bracewell RN. The Fourier transform and its applications. New York: McGrawHill, 1999.
19. Papoulis A. Signal analysis. New York. McGrawHill, 1977.
20. Turner I, Huang CL-H, Saumarez RC. Numerical simulation of paced electrogram fractionation: relating clinical observations to changes in fibrosis and action potential duration. J Cardiovasc Electrophysiol 2005;16:151–161.
21. Restivo M, Caref EB, Kozhevnikov DO, El-Sherif N. Spatial dispersion of repolarization is a key factor in the arrhythmogenicity of long QT syndrome. J Cardiovasc Electrophysiol 2004;15:323–331.
22. Kozhevnikov DO, Yamamoto K, Robotis D, Restivo M, El-Sherif N. Electrophysiological mechanism of enhanced susceptibility of hypertrophied heart to acquired torsade de pointes arrhythmias: tridimensional mapping of activation and recovery patterns. Circulation 2002;105:1128–1134.
23. Baker LC, London B, Choi BR, Koren G, Salama G. Enhanced dispersion of repolarization and refractoriness in transgenic mouse hearts promotes reentrant ventricular tachycardia. Circ Res 2000;86:396–407.
24. Papadatos GA, Wallerstein PM, Head CE, Ratcliff R, Brady PA, Benndorf K, Saumarez RC, Trezise AE, Huang CL, Vandenberg JI, Colledge WH, Grace AA. Slowed conduction and ventricular tachycardia after targeted disruption of the cardiac sodium channel gene Scn5a. Proc Natl Acad Sci U S A 2002;99:6210–6215.
25. de Bakker JM, van Capelle FJ, Janse MJ, Tasseron S, Vermeulen JT, de Jonge N, Lahpor JR. Slow conduction in the infarcted human heart. "Zigzag" course of activation. Circulation 1993;88:915–926.
26. Cabo C, Pertsov AM, Baxter WT, Davidenko JM, Gray RA, Jalife J. Wave-front curvature as a cause of slow conduction and block in isolated cardiac muscle. Circ Res 1994;75:1014–1028.
27. Kawara T, Derksen R, de Groot JR, Coronel R, Tasseron S, Linnenbank AC, Hauer RN, Kirkels H, Janse MJ, de Bakker JM. Activation delay after premature stimulation in chronically diseased human myocardium relates to the architecture of interstitial fibrosis. Circulation 2001;104:3069–3075.
28. Zhang L, Timothy KW, Vincent GM, Lehmann MH, Fox J, Giuli LC, Shen J, Splawski I, Priori SG, Compton SJ, Yanowitz F, Benhorin J, Moss AJ, Schwartz PJ, Robinson JL, Wang Q, Zareba W, Keating MT, Towbin JA, Napolitano C, Medina A. Spectrum of ST-T-wave patterns and repolarization parameters in congenital long-QT syndrome: ECG findings identify genotypes. Circulation 2000;102:2849–2855.
29. Bhandari AK, Shapiro WA, Morady F, Shen EN, Mason J, Scheinman MM. Electrophysiologic testing in patients with the long QT syndrome. Circulation 1985;71:63–71.
30. Kimbrough J, Moss AJ, Zareba W, Robinson JL, Hall WJ, Benhorin J, Locati EH, Medina A, Napolitano C, Priori S, Schwartz PJ, Timothy K, Towbin JA, Vincent GM, Zhang L. Clinical implications for affected parents and siblings of probands with long-QT syndrome. Circulation 2001;104:557–562.